A Novel Method for Illumination Suppression in Hyperspectral Images

Edward A. Ashton[a], Brian D. Wemett[a], Robert A. Leathers[b], Trijntje V. Downes[b]
[a]VirtualScopics, Inc., 500 Linden Oaks, Rochester, NY 14625;
[b]Optical Sciences Division, U.S. Naval Research Laboratory, 4555 Overlook Ave. SW, Washington, DC 20375

ABSTRACT

We have proposed a new method for illumination suppression in hyperspectral image data. This involves transforming the data into a hyperspherical coordinate system, segmenting the data cloud into a large number of classes according to the radius dimension, and then demeaning each class, thereby eliminating the distortion introduced by differential absorption in shaded regions. This method was evaluated against two other illumination-suppression methods using two metrics: visual assessment and spectral similarity of similar materials in shaded and fully illuminated regions. The proposed method shows markedly superior performance by each of these metrics.

Keywords: Hyperspectral, illumination, shadows

1. INTRODUCTION

Airborne hyperspectral imaging sensors are being increasingly used for wide-area classification and target detection applications. For example, hyperspectral imaging is used to map mineral deposits [1] [2], agricultural or forest health [3], and seagrass and coral reef health [4]. Spectral classification and target-detection algorithms for visible and short-wave infrared (SWIR) sensors rely on the ability to separate materials based on the spectral shape of their reflectivities. However, airborne sensors do not measure reflectivity directly, but instead measure spectral radiance at the aircraft altitude. Therefore, in order to apply classification algorithms, one must either attempt to model the atmosphere well enough to convert radiance-at-the-sensor to reflectance-at-the-ground or apply the algorithms directly to radiance-at-the-sensor data. We generally believe that is better to work directly with radiance data because of the difficulties with atmospheric correction methods; however, some adjustments should be made to the data to account for changes in illumination conditions.

Large-scale changes in the illumination conditions (due to changes in time of day, atmospheric conditions, or sensor altitude) can be accounted for using a linear transformation of the data referred to as the Covariance Equalization Method [5]. However, this approach, in its typical form, does not account for local variations in illumination due to shadows. Therefore, shadows from trees and buildings can have a severely adverse effect on scene classification algorithms.

The presence of shadows does not simply lower the overall magnitude of the radiance spectrum being measured; it also causes a change in spectral shape, due to the fact that the color of the light illuminating a shadowed region is different from that illuminating a sunny region.

The objective of the work presented here is to develop a practical method for identifying shadows in a scene and appropriately adjusting the illumination level and color of these areas to more closely match similar materials in the non-shadowed regions. Our proposed method is described in Section 2, some results are presented in Section 3, and our conclusions are given in Section 4.

2. METHODS

Varying levels of illumination due to shadows, varying cloud cover, etc. are a known problem for many hyperspectral segmentation and targeting algorithms. The simplest approach to this problem is to normalize the magnitude of all spectral vectors in a data cube. This process does not take into account the fact that shading does not affect different regions of the spectrum uniformly. It also reduces the effective dimensionality of the data cloud by 1 without reducing

Algorithms and Technologies for Multispectral, Hyperspectral, and Ultraspectral Imagery XIV, edited by Sylvia S. Shen, Paul E. Lewis, Proc. of SPIE Vol. 6966, 69660C, (2008) · 0277-786X/08/$18 · doi: 10.1117/12.777153

2008 SPIE Digital Library -- Subscriber Archive Copy

the actual number of dimensions, causing severe problems for any algorithm that is reliant on covariance matrix inversion.

A second approach is to convert the data from Cartesian space to a hyperspherical coordinate system. Each N-dimensional spectral vector is converted to an N-1 dimensional spectral angle. However, this approach does not account for the differential interference provided by shading.

Our approach is to convert the data from Cartesian space to a hyperspherical coordinate system. In this transformation, each *N*-dimensional spectral vector is converted to *N*-1 dimensional spectral angles and a magnitude value according to:

$$s_i = \arctan\left(\frac{v_{i+1}}{\sqrt{\sum_{j=1}^{i} v_j^2}}\right), \quad 1 \le i \le N-1. \tag{1}$$

$$s_N = \sqrt{\sum_{j=1}^{N} v_j^2},$$

where s_i is the spectral angle for band *i*, and v_i is the Cartesian coordinate for band *i*. The *N* dimension hyperspherical transformation above creates *N*-1 angles and one scalar magnitude or radius in the *N*th band. In terms of hyperspectral imagery this magnitude is the illumination value of the spectra. Figure 1 shows the two dimensional equivalent, where we have one angle θ and one magnitude *r*.

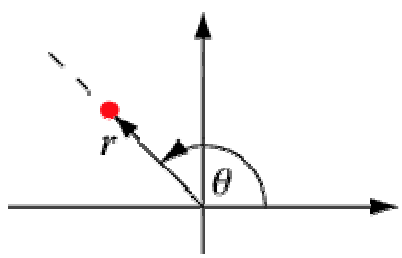

Figure 1: Polar coordinates

Similar material will have similar angles. Differences in illumination will be described mostly by the radial distance or magnitude of the hypersphere and occupy the last band in the data cube. However, it still does not account for the differential interference provided by shading.

The next step is to segment the spectra using the K-means algorithm. The resulting segmentation is largely dependent on the illumination band so a shadow map can be created by selecting the class that has the lowest magnitude values.

The edges of the shadows tend to be mixture pixels and don't need the full correction so we create a weight map that is simply the shadow map with a 3 by 3 mean filter run across it. In this way the amount of correction placed on the edges can be controlled.

The first-stage coarse correction is as follows: Let $\overline{x}_{ij}$ = current pixel, $\overline{\mu}_S$ = mean vector for all shadow pixels, $\overline{\mu}_{NS}$ = mean vector for all non-shadow pixels, $\overline{w}_{ij}$ = weight mask at pixel ij with values 1 (shadow) thru 0 (non-shadow). The corrected pixel is given by

$$\overline{x'}_{ij} = \overline{x}_{ij} * \left(\frac{(\overline{\mu}_{NS} * \overline{w}_{ij}) + (\overline{\mu}_{S} * (1 - \overline{w}_{ij}))}{\overline{\mu}_{S}} \right), \tag{2}$$

making $\overline{x'}_{ij} = \overline{x}_{ij} * \left(\frac{\overline{\mu}_{NS}}{\overline{\mu}_{S}} \right)$, when $\overline{x}_{ij}$ is in shadow and $\overline{x'}_{ij} = \overline{x}_{ij} * \left(\frac{\overline{\mu}_{S}}{\overline{\mu}_{S}} \right) = \overline{x}_{ij}$, when not in shadow. On the edges the correction will be applied in ratio to the weight map.

The main motivation for the coarse correction is to be able to better classify the shadow pixels. Each shadow pixel is assigned to one of the non-shadow classes through a simple squared error distortion measure. The second stage correction will finely adjust the shadow pixel by using the class mean of the non-shadow and shadow class. The idea is to use the angles for a particular material in non-shadow areas to guide the correction for the same material inside the shadows.

The second stage correction is applied similarly to the first stage correction: Let $\overline{x}_{ijc}$ = current pixel with classification c, $\overline{\mu}_{Sc}$ = mean vector for all shadow pixels in class c, $\overline{\mu}_{NSc}$ = mean vector for all non-shadow pixels in class c, $\overline{w}_{ij}$ = weight mask at pixel (i,j) with values 1 (shadow) thru 0 (non-shadow), the corrected pixel is given by

$$\overline{x'}_{ij} = \overline{x}_{ijc} * \left(\frac{(\overline{\mu}_{NSc} * \overline{w}_{ij}) + (\overline{\mu}_{Sc} * (1 - \overline{w}_{ij}))}{\overline{\mu}_{Sc}} \right), \tag{3}$$

making $\overline{x'}_{ij} = \overline{x}_{ijc} * \left(\frac{\overline{\mu}_{NSc}}{\overline{\mu}_{Sc}} \right)$,when $\overline{x}_{ijc}$ is in shadow and $\overline{x'}_{ij} = \overline{x}_{ijc} * \left(\frac{\overline{\mu}_{Sc}}{\overline{\mu}_{Sc}} \right) = \overline{x}_{ij}$, when not in shadow. On the edges the correction will be applied in ratio to the weight map as before.

Now that the shadow pixels are properly corrected in the shadows for illumination they can be converted back to Cartesian coordinates. The transformation is as follows:

$$v_i = R * \prod_{j=1}^{i-1} \sin(s_j), i = 1.$$

$$v_i = R * (\prod_{j=1}^{i-1} \sin(s_j)) * \cos(s_i), 2 \le i \le N-1.$$

$$v_i = R * \cos(s_i), i = N.$$

Where R is the illumination value for each pixel, s_i is the spectral angle for band i, and v_i is the Cartesian coordinate for band i.

3. RESULTS

Figure 1 shows the original image with two pixels of very similar material. One pixel is in the shadow and one is in the open. This figure highlights the problem of using spectral-based signature detection. The spectra are vastly different in and out of shadow.

Fig. 1. Intensity spectra for shadow and non-shadow pixels and locations on image

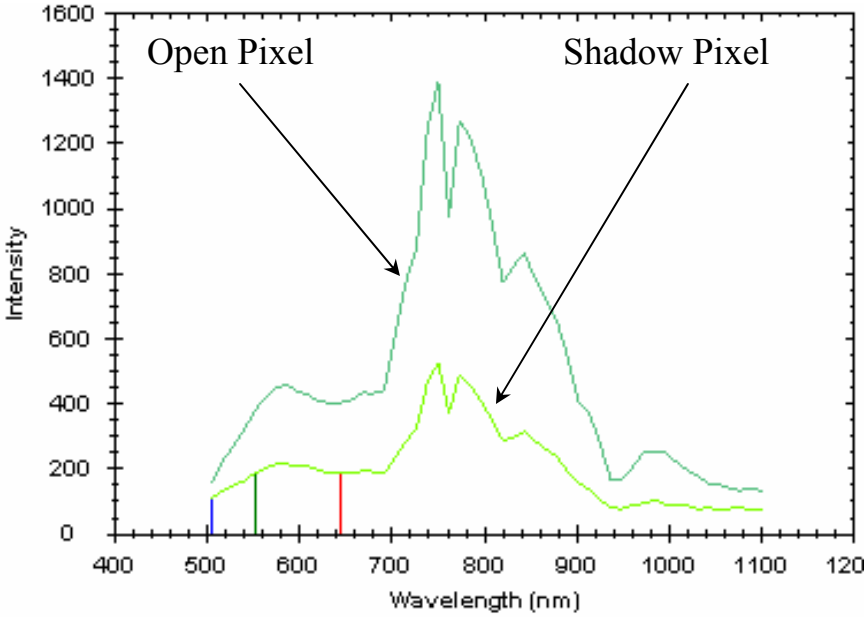

Fig. 2. Spectral signature of grass in shadow and in the open.

Figure 2 shows the spectra of the two pixels in Figure 1. Figure 3 shows the illumination image and a shadow map created by segmenting the illumination image.

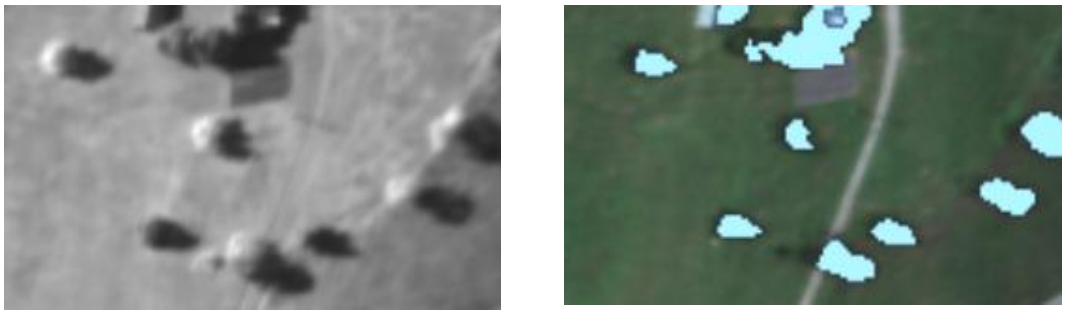

Fig. 3. Illumination image and shadow map

Figure 4 shows the results of the transformation to hypersphical coordinates [Eq. (1)]. It can be seen that the angles for the two pixels are beginning to look similar. A correction is applied to bring the shadow pixels closer to the same angles as the non-shadow pixels. The residuals of shadows can still be seen in the hyperspherical image. In the corrected image most the shadows and residuals are gone.

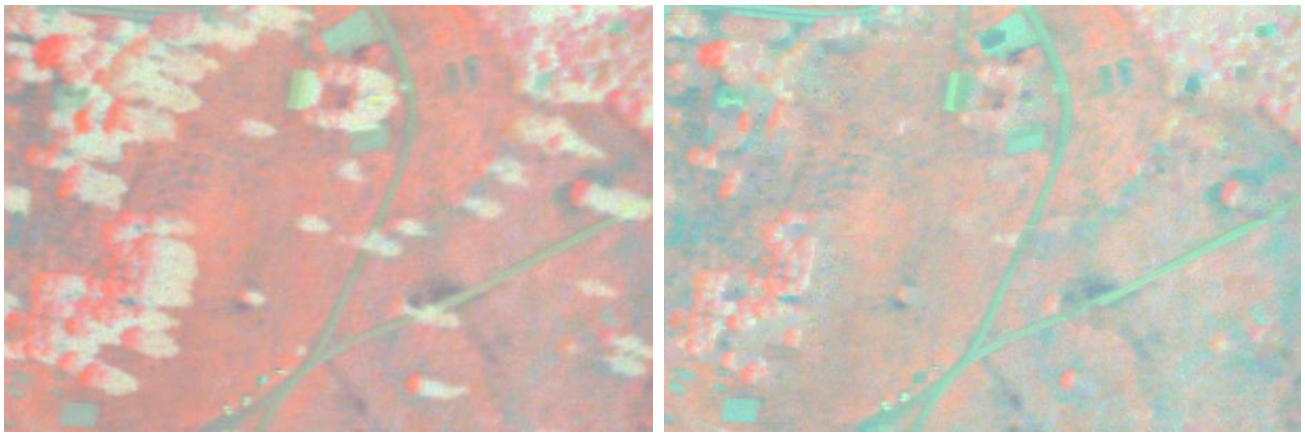

Fig. 4. Hyperspherical image and hyperspherical image with correction

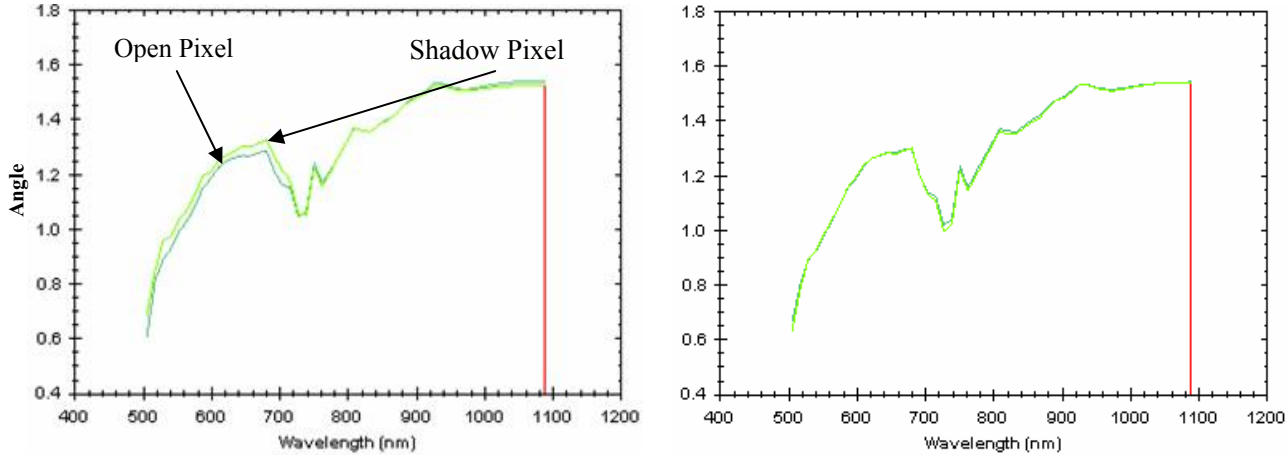

Fig. 5. Spectral angles for grass pixels in and out of shadows, before and after correction

Figure 5 shows the spectral angles of the two grass pixels in and out of shadow after hyperspherical conversion and after hyperspherical conversion with correction. The correction allows the angles of the similar material to line up very close.

The Normalized Root Mean Square (NRMS) error was computed between the two pixels for each method. The transformation only value was 0.0198, after applying the correction it was down to 0.00970.

Figure 6 shows the result of normalizing the magnitude of all spectral vectors in the data cube and the results of the corrected hyperspherical coordinates converted back to Cartesian coordinates. The shadow residuals can be seen as well as distortions in the image resulting from the loss of one dimension. The corrected image still looks realistic with the shadows removed.

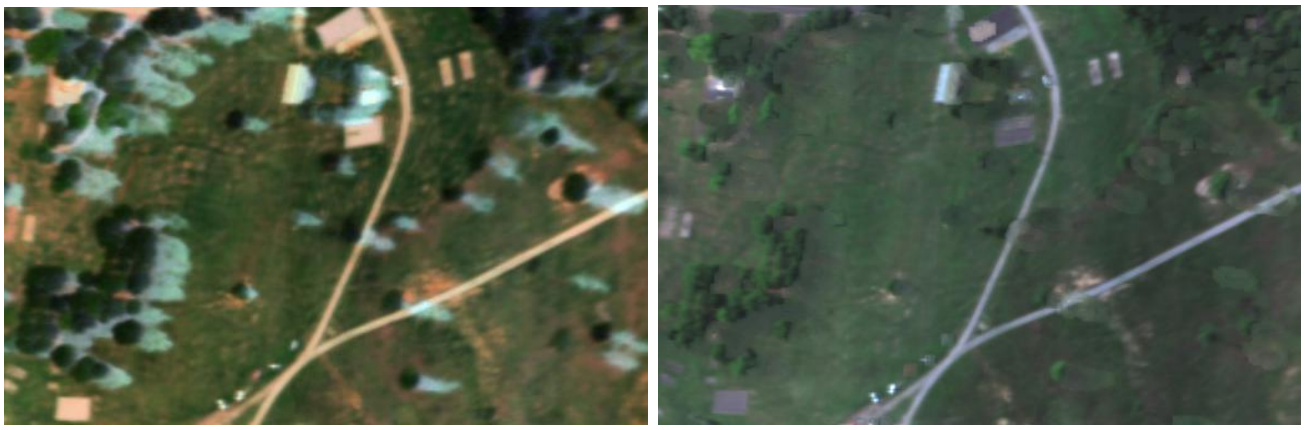

Fig. 6. Images after normalizing the magnitude of spectral vectors and image after conversion to Cartesian coordinates

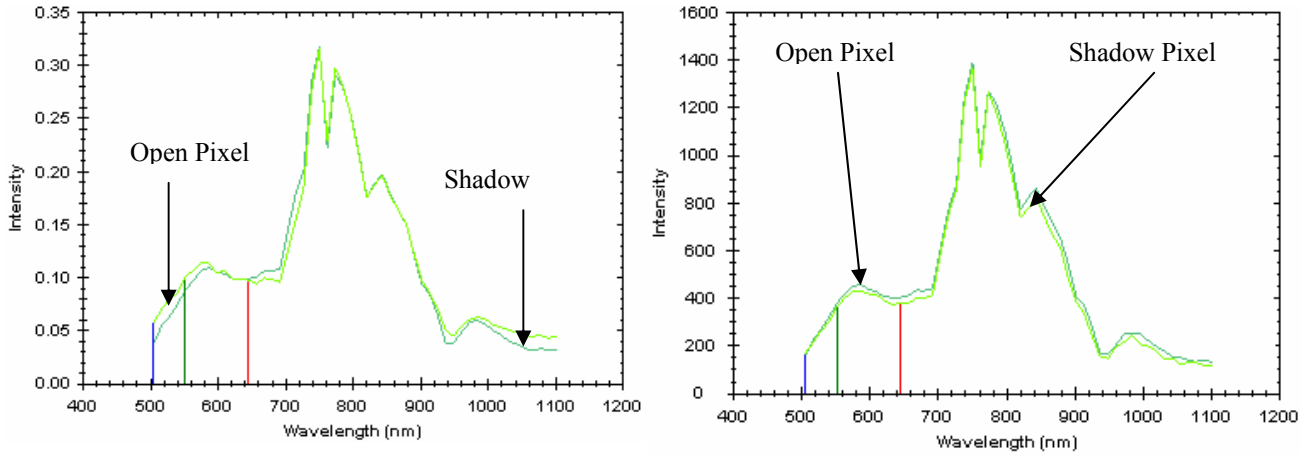

Fig. 7 Spectra resulting from normalizing the magnitude of all spectral vectors and the spectra resulting from the conversion back to Cartesian coordinates after angle correction

Figure 7 show the spectra resulting from the normalizing the magnitude of all spectral vectors and the spectra resulting from the conversion back to Cartesian coordinates after angle correction. The NRMS value calculated for the normalized magnitude method is 0.147 compared to 0.0948 for the proposed method. The signatures are closer to each other using the proposed method and we don't have the negative side effect of losing a dimension.

Figure 8 shows a blow up of the original image and the illumination-suppressed image. The tree shadows are removed with natural grass visible underneath. The entire parking lot is now visible where before it is partially in shadow. There are still some effects around the edges that need to be softened. The edge of the shadow region is being smeared out. We are currently working on these edge challenges.

Fig. 8. Original image and illumination suppressed image

4. CONCLUSIONS

The goal of this work was to develop a method for removing the effects of shadows in hyperspectral imagery. Our proposed method is to (1) convert the data to hyperspherical coordinates [Eq. (1)]; (2) classify the scene, where one of the classes defines the shadowed regions; (3) assign each pixel in the shadowed regions to one of the other classes; and (4) transform the shadowed spectra based on the means of the shadowed and unshadowed data within each class. Some care is made to account for the variation in the depth of the shade.

In our preliminary tests we found the proposed method to do a good job at correcting spectra inside shadows. This method gave better results than the two simpler methods that we tested it against. The two stage correction should ensure that materials in the shadows are corrected coarsely even if a similar material does not exist outside of shadows. These materials will not be corrected by the "fine tuning" second stage and it is yet to be determined what the detriment in detection will be. No method can completely remove the effects of shadows since the effective S/N is degraded and in deep shade the data could be unusable. However, we believe that we can do a good job of correcting for the apparent change in color and reflectivity caused by light shade.

A comprehensive detection study is needed to verify the proper correction of spectra. We also need to determine how to tell the difference between shadows and dark objects and what the impact is. We are also looking at the possibility of improving the algorithm by including spatial processing.

REFERENCES

[1] R.N. Clark, Vance, S., Livo, K.E., and Green, R.O., 1998, Mineral Mapping with Imaging Spectroscopy: The Ray Mine, AZ, Summaries of the 7th Annual JPL Airborne Earth Science Workshop, R.O. Green, ed., JPL Publication 97-21. Jan. 12-14, pp. 67-76.

[2] F.A. Kruse, Kierein-Young, K. S., and Boardman, J. W., 1990, Mineral mapping at Cuprite, Nevada with a 63 channel imaging spectrometer: Photogrammetric Engineering and Remote Sensing, v. 56, no. 1, p. 83-92.

[3] M.O. Smith et al. (2004), Use of Aerial Hyperspectral Imaging For Monitoring Forest Health, Gen. Tech. Rep. SRS–71. Asheville, NC: U.S. Department of Agriculture, Forest Service, Southern Research Station.

[4] H.M. Dierssen, R.C. Zimmerman, R.A. Leathers, T.V. Downes, and C.O. Davis (2003), "Ocean color remote sensing of seagrass and bathymetry in the Bahamas Banks by high-resolution airborne imagery", Limnol. Oceanogr. 48: 444–455.

[5] R.A. Leathers, A. Schaum, T.V. Downes (2006), "Signature evolution with covariance equalization in oblique hyperspectral imagery," SPIE Defense & Security Symposium, 17-21 April, Orlando, FL., Proc. SPIE 6233, 623307, S.S. Shen & P.E. Lewis, eds., May 2006.